CHAPTER 11

The Influence of Phase Transformations on Mantle Mixing and Plate Tectonics

W.R. Peltier,[1] S. Butler[1] and L.P. Solheim[2]

[1]Department of Physics, University of Toronto,
Toronto, Ontario, Canada M5S 1A7
[2]Department of Terrestrial Magnetism, Carnegie Institution of Washington,
5241 Broad Branch Road, N.W., Washington, D.C. 20015 USA

Several recent analyses of the process of mantle convection have demonstrated the profound influence that the solid-solid phase transformations that bracket the mantle transition zone may have on radial mixing. The only available results to date from spherical models configured with a Rayleigh number appropriate to the modern Earth are those recently published by Solheim and Peltier (1994a,b). These results demonstrate that the episodicity of radial mixing in these simulations is controlled by the creation and destruction of a thermal boundary layer that envelops the endothermic phase transformation at 660 km depth. Diagnostic analyses of the simulations suggest that a local Rayleigh number characteristic of the boundary layer may be defined which exceeds a well defined critical value prior to occurrence of the avalanche events which themselves develop subsequent to the onset of boundary layer instability. The analyses presented herein have been performed to explain why a critical condition of this kind should arise and to explore the possible implications of the episodically layered mode of convection for understanding of the so-called "supercontinent cycle" of continental accumulation and dispersal.

1. Introduction

The radial structure of the mantle general circulation, in particular the question as to whether this structure is layered or whole mantle in style, is determinant of a wide range of properties of the planet. Principal among these is undoubtedly the rate of core cooling which has profound implications both for the "lifetime" of the magnetic field and for the mechanism of its maintenance against Joule dissipation. Of comparable importance, however, are the implications of the style of convective mixing for our understanding of the processes of continental drift and seafloor spreading. Until rather recently (e.g. as reviewed in Peltier and Jarvis, 1982) there has been no consensus as to whether the style of convection was whole-mantle or layered as several arguments could be marshalled on either side of the debate. An inadequate but adequately brief (!) summary of this (until recently) prevailing circumstance must begin by pointing to the issue of the mechanism whereby layering could be supported if indeed it were to exist at all. Three possible mechanisms that might lead to layering of the circulation have at various times been suggested: namely (I) a large increase of viscosity at 660 km depth, (II) an increase of mean atomic weight across the 660 km horizon and finally (III) the influence of the pressure induced phase transformation that occurs at 660 km depth and which marks the base of the so-called transition zone of the mantle. Concerning the plausibility of mechanism I, Peltier (1972) showed that a viscosity increase by at least two orders of magnitude would be required to effect

dynamical stratification of the circulation by this means and Peltier (1974 and subsequent) and Cathles (1975) demonstrated that post-glacial rebound observations entirely ruled out a viscosity contrast of this magnitude. Concerning the plausibility of mechanism II, which was strongly favoured by a number of early analysts (e.g. Richter and McKenzie, 1981; Jeanloz and Thompson, 1983), the laboratory phase equilibrium measurements of Ito and Takahashi (1989) established rather clearly that no increase of mean atomic weight across the 660 km discontinuity was required to explain the seismological properties (e.g. reflectivity and inferred density increase) that are characteristic of this depth horizon. Mechanism III, on the other hand, which had been mentioned by Richter and McKenzie (1981) as a possible alternative to chemical layering, was first analysed in an attempt to quantify its effectiveness by Christensen and Yuen (1984, 1985) who suggested that no significant influence would occur if the Clapeyron slope for the endothermic transition were less (in magnitude) than about –6 $MPa^{\circ}K^{-1}$. Given that the measurements of Ito and Takahashi (1989) constrained the Clapeyron slope for the transition from Spinel to a mixture of Perovskite and Magnesiowüstite to be near –4 $MPa^{\circ}K^{-1}$ it therefore seemed that mechanism III would also be ineffective.

If there were no evidence suggesting that some degree of layering of the circulation must exist, one might reasonably expect that the above arguments would have sufficed to settle the issue definitively. However data in favour of some degree of layering includes at least one type which has survived serious attempts to undermine it. This data is of a geochemical nature. Although very forcefully presented earlier geochemical arguments in favour of layered convection, based upon trace element geochemistry of the Sm-Nd system (O'Nions *et al.*, 1979; Wasserburg and DePaulo, 1979), have since been shown to be equivocal, the implications of the additional data would appear to be harder to refute. These data involve the present day observed rate of ^3He loss from oceanic ridges as well as *Ar* concentration measurements (e.g. O'Nions and Tolstikhin, 1994) and has been interpreted to require a high degree of chemical segregation of the upper mantle and transition zone from the lower mantle. That this scenario is in fact dynamically plausible, in spite of the above cited arguments that would appear to rule out mechanisms I–III, has been demonstrated only recently and is connected to a flaw in the argument against mechanism III.

In the open literature, the possibility of the existence of such a flaw became evident with the publications of Machetel and Weber (1991) and Peltier and Solheim (1992). Working in axisymmetric spherical geometry these groups both performed simulations of the impact of mantle phase transitions upon the convective mixing process using the Ito and Takahashi (1989) data to constrain the Clapeyron slope of the endothermic phase transition at 660 km depth. The calculations of Machetel and Weber (1991) included only the endothermic transition at 660 km depth and were performed at a maximum value of the Rayleigh number of 2×10^6, the same maximum Rayleigh number as had been achieved in the Cartesian geometry calculations of Christensen and Yuen (1985). Nevertheless, with a Clapeyron slope of –4 $MPa^{\circ}K^{-1}$ significant layering was observed to develop in the simulated flows, a degree of layering that should not have arisen if the analyses of Christensen and Yuen had been accurate. The simultaneously produced analyses of Peltier and Solheim (1992) very strongly reinforced the idea that the analyses of Christensen and Yuen were flawed. These analyses were performed at the considerably higher Rayleigh number of 10^7, which is characteristic of the modern earth, and suggested the occurrence of much more intense

layering for a significantly lower Clapeyron slope (–2.8 MPa°K^{-1}) than had been revealed by the lower Rayleigh number analyses of Machetel and Weber (1991). Also included in the simulations of Peltier and Solheim (1992) was an accounting of the influence of the exothermic Olivine-Spinel transition that occurs at a depth of 400 km and this was shown, as expected on physical grounds, to slightly decrease the effectiveness of the deeper endothermic transition in inducing layering.

More recent and detailed analyses than these earliest contributions have since been reported by Tackley *et al.* (1993), Honda *et al.* (1993), Weinstein (1993), Solheim and Peltier (1994a,b) and Tackley *et al.* (1994). In particular a full discussion of the sensitivity of the degree of layering to changes in each of the main control parameters was presented in Solheim and Peltier (1994a,b), whose results were verified in detail by Tackley *et al.* (1994) who employed a three dimensional spherical model rather than the axisymmetric spherical geometry of Solheim and Peltier (1994a,b). The computational demands of the three dimensional simulations were, however, such that Tackley *et al.* were restricted to the same maximum Rayleigh number as that which was achieved by Machetel and Weber (1991) in their axisymmetric analyses, namely $Ra \approx 2 \times 10^6$.

Our goal in the present discussion will be to extend the analyses of Solheim and Peltier (1994a,b) in two specific ways, one quantitative, the other qualitative. The quantitative extension will consist of an analysis of the physical processes that determine the critical value of the internal boundary layer Rayleigh number that appears to govern the occurrence of the avalanche events which themselves control the efficiency of mixing through the 660 km endothermic phase transformation when the system Rayleigh number is near the earth-like value of 10^7. The qualitative extension, on the other hand, will involve a discussion of the important role that phase transition mediated intermittency may play in the so-called "supercontinent cycle" of continental accumulation and dispersal. In the following section 2 of this paper we shall begin by reviewing the theoretical model of phase transition mediated convection that we have developed and the main results that have been obtained using it. In section 3 we focus upon the internal thermal boundary layer that straddles the endothermic phase transformation in the layered state and employ linear stability methodology to attempt to explain the critical value of the boundary layer Rayleigh number that governs the occurrence of the avalanche process. Section 4 is devoted to a discussion of the possible importance of the avalanche process to the understanding of supercontinent agglomeration and breakup. Our concluding remarks are presented in section 5.

2. An *A Priori* Model of the Influence of Phase Transformations on Convective Mixing: Theoretical Structure and Representative Results

Because the dominant mineralogical constituent of the planetary upper mantle (at depths shallower than 400 km) is Olivine ($Mg_{1-x}Fe_xSiO_4$) with the iron fraction $x \approx 0.1$, the phase diagram of this material is clearly of considerable importance to the understanding of internal structure. It has been known for some time (e.g. Ringwood and Major, 1966; Akimoto and Fujisawa, 1966) that Olivine transforms to the Spinel phase at depths greater

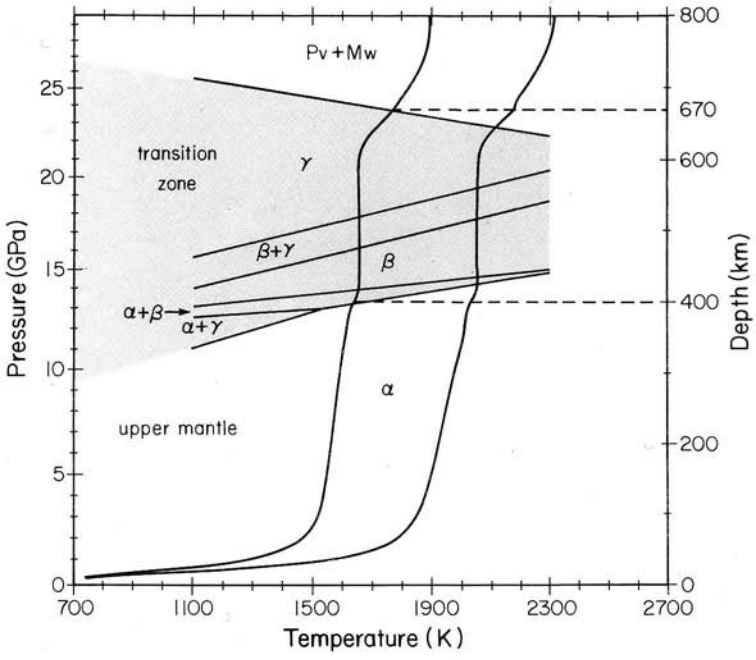

Figure 1. Phase boundaries for the $\alpha \rightarrow \beta \rightarrow \gamma$ transitions of $(Mg_{0.89}Fe_{0.11})_2SiO_4$ (thin solid lines) are overlain on two model geotherms (heavy solid lines). The phase boundaries are from Akaogi *et al.* [1989] and the geotherms are from two convective mixing simulations performed with the multiphase convection model with $Ra = 10^7, \beta_1 = +3.0$ MPa/°K and $\beta_2 = -2.8$ MPa/°K. In one simulation there was no internal heating (low temperature geotherm), while in the other (high temperature geotherm), internal heating with $\mu = 10$ was employed which corresponds approximately to 50% heating from within and 50% heating from below.

than 400 km and that this transformation defines the top of the "transition-zone". As pressure further increases and following a sequence of secondary reactions the Spinel phase itself is eventually transformed to a mixture of Perovskite $(Mg,Fe)SiO_3$ and Magnesiowüstite MgO. This occurs at the depth of 660 km (Ito and Takahashi, 1989) and leads to the creation of the sharp seismic discontinuity that defines the base of the transition zone, below which is the lower mantle. From this horizon to the core-mantle interface at a depth of 2880 km there appear to be no further transformations of phase although debate continues on this issue. Figure 1 shows a schematic of the shallowest part of the Olivine phase diagram (after Ito and Takahashi, 1989). Inspection of this diagram shows that the Olivine-Spinel transition is exothermic in that its Clapeyron slope dp/dT is positive with 2 MPa°$K^{-1} \leq dp/dT \leq 3$ MPa°K^{-1} whereas the Spinel-post Spinel transition is endothermic with –6 MPa°$K^{-1} \leq dp/dT \leq -2$ MPa°K^{-1}. As we will see, it is the endothermic nature of the latter transition that causes its interaction with the convective mixing process to lead to such interesting effects. In assessing the possible importance of

these effects, however, we must keep clearly in view that fact that the Olivine fraction constitutes only about 60% of the mineralogical constituents of the upper mantle and transition zone so that the behaviour of the remaining material through the Spinel-post Spinel transition will be seen to be of considerable importance. We will return to this point below.

In order to analyse the impact of these phase transformations on convective mixing we have developed a mathematical model which is embodied in the following respective non-dimensional forms of the conservation laws for mass, momentum and internal energy.

$$\underline{\nabla} \cdot (\rho_r \underline{u}) = 0 \tag{1}$$

$$0 = -\rho g \hat{r} - \underline{\nabla}_p + \alpha_0 T_c \left\{ \underline{\nabla} \times \underline{\nabla} \times \underline{u} + \frac{4}{3} \underline{\nabla} \cdot \mathbf{u} \right\} \tag{2}$$

$$\frac{DT}{Dt} + \tau u_r (T + T_0) = \frac{1}{Ra} \left\{ \nabla^2 T + \frac{1}{K} \frac{dK}{dr} \frac{\partial T}{\partial r} \right\} + \frac{\mu}{C_p Ra} + \frac{\tau_0 \Phi}{\rho_r C_p} + \frac{\tau_0}{\alpha_0 T_c C_p} \frac{D}{Dt} \{ \ell_1 \Gamma_1 + \ell_2 \Gamma_2 \} \tag{3}$$

in which we have assumed constant viscosity but allowed for depth dependent thermal diffusivity κ. This system is closed with an equation of state that may be adequately approximated as:

$$\rho = \rho_r \left\{ 1 - \alpha_0 T_c \alpha (T - T_c) + \frac{1}{K_T} (p - p_r) \right\} + \Delta_1 (\Gamma_1 - \Gamma_{r1}) + \Delta_2 (\Gamma_2 - \Gamma_{r2}) \tag{4}$$

with the phase density functions Γ_i defined as:

$$\Gamma_i = \frac{1}{2} \left\{ 1 + \tanh \left[(r_{pi}(\underline{x}, t) - r) \frac{h_i}{d} \right] \right\} \tag{5}$$

in which the radial position of the i^{th} phase boundary r_{pi} is carried as a prognostic variable in the model, h_i is the thickness of the divariant phase loop of the i^{th} phase transition and d is the depth of the mantle, the length scale employed to develop the non-dimensional forms of the field equations. In the above, $\underline{u}$ is the vector velocity field, u_r is its radial component, Φ is the dissipation function (Peltier, 1972) and T_c is the reference temperature.

In the momentum balance equation (2) it will be noticed that the inertial force has been eliminated from the left-hand-side, a consequence of the fact that it scales as the ratio of the Rayleigh number to the Prandtl number ($Pr = \nu/\kappa$) and the latter is effectively infinite for the planetary mantle. Furthermore, in the continuity equation (1) we have dropped the partial time derivative of the density field thus leading to the so-called anelastic approximation of the influence of compressibility. This approximation is exceedingly accurate for the mantle because of the extremely low Mach number that is characteristic of mantle flow. In the

energy equation (3) the compression work term which scales as the dissipation number τ (Peltier, 1972) has been approximated by representing the material derivative of the pressure field Dp/Dt as $u_r dp_r/dr$ where p_r is the depth dependent pressure field in the hydrostatic background state which has $p = p_r(r)$, $\rho = \rho_r(r)$ and $T = T_0(r)$. The main control variables in the above nondimensional system are the Rayleigh number

$$Ra = \frac{\alpha_0 T_c g_0 d^3}{\kappa_0 \nu_0}, \tag{6}$$

the dissipation number

$$\tau_0 = \frac{g_0 \alpha_0 d}{C_p}; \quad \tau(r) = \tau_0 \frac{g\alpha}{C_p} \tag{7}$$

and the non-dimensional heating rate per unit mass

$$\mu = \frac{\rho_0 \chi d^2}{\kappa_0 T_c} \tag{8}$$

The subscript zero, wherever it appears in the above equations, denotes a reference value of the parameter to which it is attached. The symbols ρ, g, α, T, K, C_p and K_T respectively denote density, gravitational acceleration, coefficient of thermal expansion, temperature, thermal conductivity, specific heat capacity at constant pressure and isothermal compressibility. χ is the rate of internal heating per unit mass. The interested reader will find the details of the nondimensionalization procedure more fully described in Solheim and Peltier (1990, 1994a).

The main distinction between the model embodied in the above system of partial differential equations and the models that have recently been employed by others to investigate the impact of pressure induced phase transitions on mixing is connected with the explicit way in which this physics is described in our model. Rather than representing the influence of the individual phase transformations "implicitly" through local modifications of α and C_p as in Christensen and Yuen (1984, 1985) and Tackley *et al.* (1993, 1994) we treat this physics explicitly on the basis of the assumption that the Clapeyron slopes of the individual transitions are either constant or known functions of temperature. For present purposes, assuming $dp/dT = \beta_i$ = constant for the i^{th} transition ($i = 1$ representing the Olivine-Spinel transition and $i = 2$ representing the Spinel-post Spinel transition) we may integrate the individual Clapeyron equations to write:

$$p = p_{0i} + \beta_i (T + T_0) \tag{9}$$

where, as previously, T_0 is the reference temperature. Now clearly the β_i are not independent of the latent heats of reaction ℓ_i but rather are related by the Clapeyron equation

$$\beta_i = \frac{\rho^2 \ell_i}{\Delta_i (T + T_0)} \tag{10}$$

in which ρ is the density of the anelastic reference state at the position of the i^{th} phase boundary and Δ_i is the density jump. In our model the integration of the differential system

(1)–(5) is considerably simplified through introduction of the transformed "temperature" A, defined as:

$$A = T - \frac{\tau_0}{\alpha_0 T_c C_p}(\ell_1 \Gamma_1 + \ell_2 \Gamma_2) \tag{11}$$

since this reduces (3) to an equation which requires the advection of only a single quantity. In terms of this new dependent variable equation (9) then delivers the following two simultaneous equations in the radial positions $r_{p1}(\theta)$ and $r_{p2}(\theta)$ of the two phase boundaries.

$$\beta_1 \left\{ A + T_0 + \frac{\tau_0}{2\alpha_0 T_c C_p}[\ell_1 + \ell_2 + \ell_2 \tanh(r_{p2} - r_{p1})h_2] \right\} + p_0 - p_r = 0 \tag{12a}$$

$$\beta_2 \left\{ A + T_0 + \frac{\tau_0}{2\alpha_0 T_c C_p}[\ell_1 + \ell_2 + \ell_1 \tanh(r_{p1} - r_{p2})h_1] \right\} + p_0 - p_r = 0 \tag{12b}$$

At each time step in the numerical integration of the model system we solve (12a) and(12b) to obtain the new positions of the phase boundaries. In axisymmetric spherical geometry these radial locations are clearly functions of latitude as well as time. As will be made clear in what follows, the accurate computation of the time variation of the positions of these phase boundaries is extremely important to the accurate representation of phase boundary effects. It is for this reason that we have considered it advisable to compute these positions explicitly rather than to incorporate them implicitly through introduction of a sheet mass load determined by appeal to a locally modified value of the coefficient of thermal expansion α.

Since the original analysis of phase transition effects on convective mixing by Busse and Schubert (1971) and the application of this work to the case of the mantle (e.g. Peltier, 1972; Schubert *et al.*, 1975), it has been well understood that such influence arises from two fundamental effects, namely latent heat release and phase boundary deflection. Whether the phase transition of interest is exothermic or endothermic these two effects always contribute oppositely in their influence on the convective circulation. Furthermore the issue as to which effect is dominant will depend upon the strength of the circulation which is itself determined primarily by the Rayleigh number defined in equation (6) above. In the limit of small "amplitude" of convection the relative strength of these two competing effects is determined (e.g. Peltier, 1985) by the two non-dimensional parameters:

$$R_\ell = \frac{g_0 \alpha_0 d^3 \ell_i}{\kappa \nu C_p} \tag{13a}$$

$$S = \frac{\Delta_i / \rho}{d\alpha_0 \left(\frac{g_0 \rho}{\beta_i} + \frac{dT_0}{dr} \right)} \tag{13b}$$

Because the parameter R_ℓ, which measures the influence of latent heat release, scales as the cube of the thickness of the layer within which the phase transition is located, whereas

the parameter S, which measures the importance of phase boundary deflection in the small amplitude theory, scales inversely as d itself, it will be clear that the relative importance of the two competing effects will depend upon the thickness of the layer within which a phase transition of given strength is situated. The linear stability analyses of Schubert *et al.* (1975) were based upon the assumption that the thickness of the convecting layer was approximately equal to the depth to the base of the transition zone. Their analysis then suggested that the influence of phase boundary deflection was dominant, an effect which is stabilizing for an endothermic transition. This choice of scaling does not, of course, situate the phase transition in a geometry which is matched to that of the planetary mantle. In Peltier (1985) this mismatch was discussed explicitly and it was shown that when a length scale d equal to the thickness of the mantle was employed then the impact of the endothermic phase transition, being now dominated by the effect of latent heat release, as measured by R_ℓ, was strongly destabilizing. Clearly therefore, if the endothermic phase transition is to be stabilizing this must arise as a consequence of finite amplitude effects associated with the fact that the influence of phase boundary deflection rises more quickly with the Rayleigh number Ra than does the influence of latent heat release. This fact has been very clearly born out by the recently presented results from the direct numerical integration of the system represented by equations (1)–(12).

By way of illustrating the main results that have been obtained through such analyses we will begin by showing in Figure 2 the results of an integration that has been performed for a value of the Rayleigh number $Ra = 10^7$, a value which is very close to that which is characteristic of the modern Earth. For the purpose of this calculation the Clapeyron slopes of the exothermic and endothermic transitions have been fixed to the values of $\beta_1 = 3$ MPa°K^{-1} and $\beta_2 = -2.8$ MPa°K^{-1} in accord with the previously cited experimental determinations. On Figure 2, the results of the integration are shown for a period of 1.25 billion years with the zero of time fixed to an instant sufficiently long after the beginning of the actual numerical integration that the starting transient has died away. Three diagnostic time series from the integration are shown, respectively for the mean (volume averaged) internal temperature of the model mantle $\overline{T}(t)$, for the average magnitude of the "horizontal" component of velocity at the planets surface $\langle |u_{\rm sur}| \rangle (t)$, and for the azimuthal average of the mass flux across the two phase transition horizons, computed according to the definition (in which $r_{\rm cmb}$ is the radius of the core-mantle boundary and $r_{\rm sur}$ is radius of the planetary surface):

$$F_m(r,t) = \frac{\langle \rho_r |u_r| \rangle}{\left[\dfrac{1}{(r_{\rm sur} - r_{\rm cmb})} \cdot \displaystyle\int_{r_{\rm cmb}}^{r^{\rm sur}} \langle \rho_r |u_r| \rangle dr \right]} \tag{14}$$

The results are shown for a calculation that included no internal heating ($\mu = 0$).

Inspection of the diagnostic time series on Figure 2 shows that in this case the nature of the circulation is highly "intermittent", with relatively brief episodes of warming of the shell interior, rapid horizontal motion at the surface and high mass flux across the phase boundaries separated by relatively long intervals of cooling, slow surface motion and lower mass flux across the 660 km endothermic transition than across the shallower exothermic transition. Since the depth dependent mass flux diagnostic (14), originally suggested in

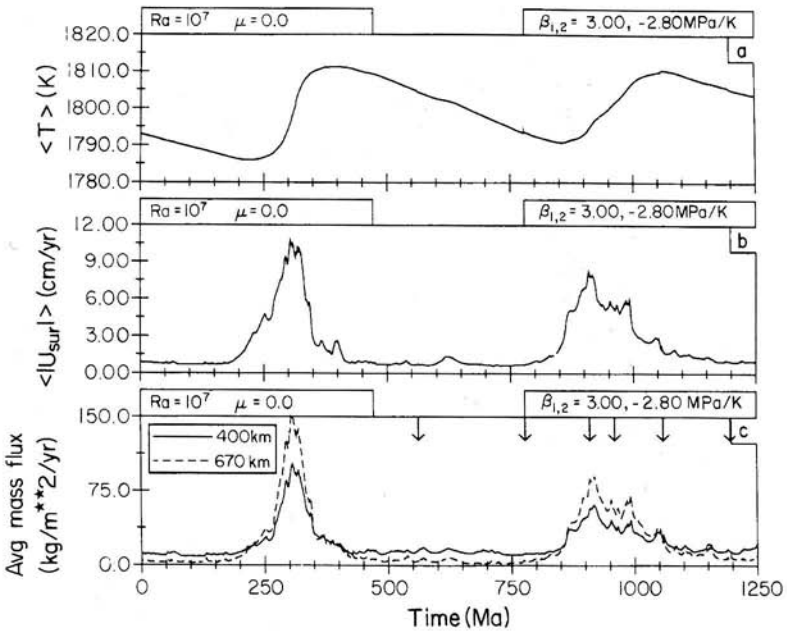

Figure 2. Time series of (a) mean mantle temperature, (b) mean surface speed and (c) dimensional mean absolute mass flux through the phase transition interfaces at 400 km and 670 km depth. All three time series were generated from a simulation with $Ra = 10^7$, $\mu = 0$, $\beta_1 = +3.0$ MPa/°K, $\beta_2 = -2.8$ MPa/°K and $h_1 = h_2 = 200$. The arrows in (c) denote the instants of time for which the temperature field data are shown in Figure 3 below.

Peltier and Solheim (1992), is clearly of parabolic form in the absence of phase transition effects, the circumstances in which the mass flux at 660 km depth is less than that at 400 km depth are clearly circumstances in which the flow is quite strongly layered.

The layered nature of the flow that obtains during the intermittent episodes of strong mixing is demonstrated explicitly in Figure 3 which displays colour maps of the temperature field at the six times marked by arrows in part (c) of Figure 2, a sequence of times which encompass the second of the two strong mixing events. Inspection of the individual frames in this sequence demonstrates the strongly layered nature of the flow that obtains at 780 Ma prior to the onset of intense mixing. Hot material rising in plumes driven by instability of the lower boundary layer adjacent to the cmb reaches the 660 km discontinuity but does not penetrate this horizon. By 910 Ma, however, which is the time of most intense mixing according to the diagnostic time series in Figure 2, intense cold downwellings are seen to penetrate this level, forming what might reasonably be called "avalanche" events (as described in Solheim and Peltier, 1994a). Simultaneously with the occurrence of these intense downwellings it will be observed that there is a strong enhancement of heat flux across the cmb, thus accounting for the increase of mean temperature previously described

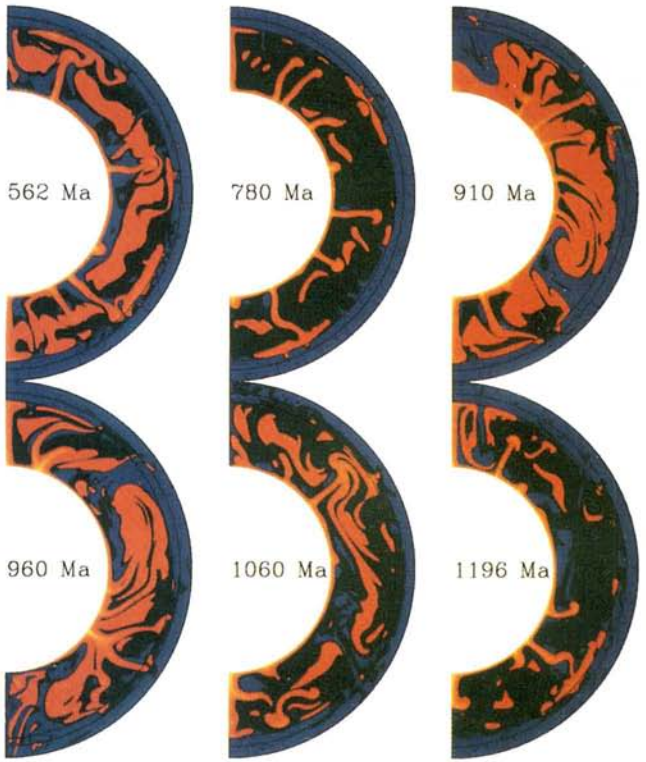

Figure 3. Colour maps of the mantle temperature field for the six instants of time shown on plate (c) of Figure 2 which bracket an episode of avalanche activity in the spherical axisymmetric model. The colour scale spans the range $300^{\circ}\mathrm{K} \leq T \leq 3700^{\circ}\mathrm{K}$, the higher temperature corresponding to that of the cmb and the lower to the Earth's surface.

in reference to part (a) of Figure 2. At 960 Ma the cold avalanche events are still active but by 1196 Ma, the last time in the sequence of temperature fields shown on Figure 3, the flow has once more returned to the layered state that existed at 780 Ma.

The manner in which the phase transitions effect the layered state of flow and further characterizations of the layering itself are provided by the flow diagnostics shown in Figure 4. This figure shows temporally averaged depth dependent mass flux functions for 4 intervals of time (plate a), depth dependent geotherms for models which differ from one another only in the magnitude of the Clapeyron slope of the endothermic phase transition (plate b) and depth dependent lateral heterogeneity spectra (plate c). The series of mass flux functions shown on plate (a) demonstrate that the flux across 660 km depth is strongly suppressed during the intervals of time corresponding to the quiescent layered states that separate intervals of avalanche activity, as must be the case if the flow were indeed layered. Inspection of plate (b) of this Figure demonstrates, in terms of long timescale averaged

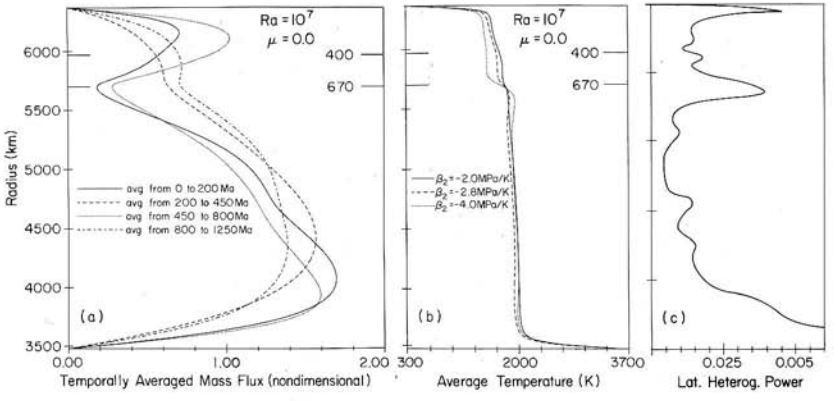

Figure 4. (a) Azimuthally and temporally averaged mass flux across the 670 (660) km seismic discontinuity from 4 intervals of time for the simulation from which temperature fields are shown on Figure 3. (b) Azimuthally and temporally averaged geotherms from three heated from below convection simulations which differ only in the value assumed for the Clapeyron slope of the 670 (660) km phase transformation. (c) Depth dependent lateral heterogeneity power spectrum (time averaged) from a heated from below convection model at $Ra = 10^7$. Note the sharp peak in the spectrum that is predicted to be coincident with the Spinel-post Spinel phase transformation.

geotherms, that the more strongly the flow is layered by the action of the endothermic transition (i.e. the larger the Clapeyron slope) then the stronger is the thermal boundary layer that develops across the endothermic horizon. In plate (c) is shown the depth dependent temperature field variance for the standard heated from below model and this reveals that a strong peak in the variance spectrum develops within the thermal boundary layer that straddles the endothermic phase transition when the flow is in the layered state. Since its first description in Peltier and Solheim (1992) this feature has come to be recognized as one which might be of use by seismologists as a means of testing whether or not the phase transition effect predicted by the hydrodynamic models actually operates in the "real" earth.

Although these diagnostic characterizations of the phase transition effect are useful they clearly do not suffice to adequately explain the physical mechanism through which the intermittency of the circulation is sustained. Some insight into this underlying mechanism is provided by Figure 5, which on plate (a) reproduces the 670 km mass flux time series from the simulation employed to produce Figure 2. Also shown on Figure 5 are time series for two characteristics of the 660 km thermal boundary layer that develops across the endothermic phase transition interface. These consist of the temperature drop across the boundary layer (averaged in azimuth), ΔT_{670}, and the boundary layer thickness, δ_{670}. On the basis of these two time dependent characterizations of the circulation one may form a boundary layer Rayleigh number

$$Ra_\delta(t) = \frac{g_0 \alpha_0 \Delta T \delta^3}{\kappa_0 \nu_0} \tag{15}$$

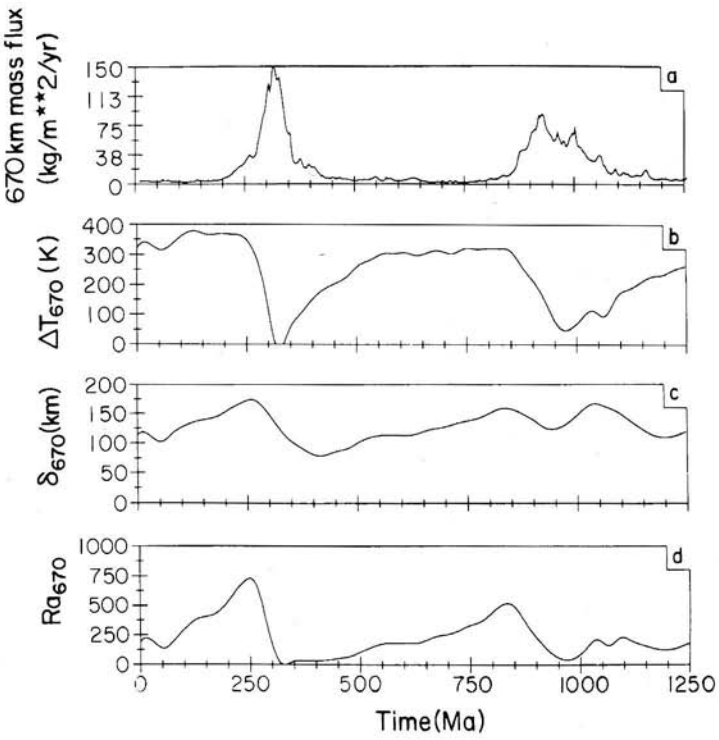

Figure 5. Four diagnostic time series from a heated-from-below convection model with multiple phase transitions. (a) Radial mass flux across 670 km depth, (b) temperature contrast across the 670 km thermal boundary layer, (c) thickness of the 670 km thermal boundary layer and (c) the boundary layer Rayleigh number.

in which the remaining parameters are the same as those which appear in the definition of the system Rayleigh number itself in (6). The time series $Ra_\delta(t)$ is shown in plate (d) of Figure 5. Comparison of this time series with that for the 670 km mass flux shown in plate (a) demonstrates that *prior* to the occurrence of the two major avalanche episodes the boundary layer Rayleigh number achieves a maximum value between 500 and 750. *After* the boundary layer Rayleigh number begins to fall the 670 km mass flux rises rapidly. As suggested in Solheim and Peltier (1994a) this sequence of events is most easily understood by interpreting the avalanche episodes as arising from instability of the internal thermal boundary layer that is caused to develop across the endothermic phase transition because of the mass flux inhibiting effect of phase boundary deflection. If this were the correct interpretation of the origin of the intermittency that characterizes mantle mixing in the presence of the endothermic transition, then it should be possible to explain the numerically obtained critical value for the boundary layer Rayleigh number above which instability of the layered circulation occurs. This issue is addressed in the following section.

3. Linear Stability of the Internal Mantle Boundary Layer

We begin this analysis by re-stating the well known set of first order perturbation equations that describe the evolution of small amplitude fluctuations superimposed upon a basic state that we assume to be at rest and which is characterized by a variation of temperature with depth only that has the form of the time averaged geotherms shown in plate (b) of Figure 4 which contain the internal boundary layer at 670 km depth. This set of perturbation equations may be written (in the first instance), following the usual procedures, in the form

$$\frac{d\underline{Y}}{dr} = \underline{\underline{A}}\,\underline{Y}, \tag{16}$$

in which the solution vector $\underline{Y} = (w, w', w'', \Pi/\mathbf{A}, \Theta, \Theta')$, w is the perturbation radial velocity, $\Pi/\mathbf{A}$ is the scaled pressure fluctuation, Θ is the temperature perturbation and the prime indicates radial differentiation. The matrix of coupling coefficients $\underline{\underline{A}}$ is a function of the system Rayleigh number Ra defined in (6) and of spherical harmonic degree ℓ (say), if the stability analysis is to be performed in spherical geometry, or of horizontal wavenumber k (say) if the analysis is to be performed in Cartesian geometry. The neutral stability boundary which separates regions in the (Ra, ℓ) plane within which small amplitude fluctuations are amplified from the region in which they are quenched is determined by solving the two-point boundary value problem posed by (16) coupled with appropriate boundary conditions at the locations equivalent to the cmb and the Earth's surface. The boundary conditions we shall apply at these endpoints will be taken to be those appropriate to impermeable and free slip conditions. At the locations of the phase transitions, following the original analyses of Busse and Schubert (1971) and using the nondimensionalization scheme of Peltier (1972) we must apply jump conditions on the temperature perturbation and on the pressure fluctuation. The magnitudes of the discontinuities in these variables depend upon the non-dimensional parameters R_ℓ and S defined previously in (13a) and (13b) and are given by:

$$\Theta_2 - \Theta_1 = \frac{1}{r} R_\ell w(r) \tag{17a}$$

$$\frac{\Pi_2}{A} - \frac{\Pi_1}{A} = S\Theta \tag{17b}$$

As mentioned previously the mathematical structure embodied in (16) and (17a,b) has been employed in Peltier (1972, 1985) to analyse the situation in which the exothermic and endothermic transitions are assumed to be located in a mantle in which the radial variation of temperature consists of the conduction solution for the shell (in spherical geometry) or layer (in Cartesian geometry). Here our intention is to address in a preliminary way the circumstance in which a region of strong temperature gradient exists only in a thin region surrounding the endothermic horizon as defined by the geotherms for intermittently layered convection shown previously on Figure 4b. In the absence of the phase transition it is well known (e.g. Howard, 1962) that the stability boundary is "degenerate" in the sense that the critical Rayleigh number for the onset of convection tends uniformly to zero in the limit of zero wavenumber (infinite wavelength) if the boundaries are removed to infinity. This

is simply a consequence of the fact in the absence of the stabilizing influence of boundary proximity no finite vertical temperature gradient in a motionless fluid is sustainable. This being the case and it also being the case that at small convection amplitude the influence of the endothermic phase transition is to destabilize the layer, as mentioned above, how could it be that a non-zero critical boundary layer Rayleigh number could govern the onset of the avalanche events as suggested in the last section in connection with the interpretation of Figure 5.

To understand the reason for this we must clearly include a more complete description of the environment within which the internal thermal boundary layer develops. We submit that it is a vital property of this environment that a convergence of mass exists over a substantial horizontal scale across the phase transition interface whose radial deflection (in the full nonlinear dynamics) is responsible for inducing the layered flow. This convergence, which we may represent by a radial variation of background radial (vertical) velocity dw_0/dr, say, leads to a modification of the usual stability matrix $\underline{\underline{A}}$ in (16) into the form:

$$\underline{\underline{A}} = \begin{pmatrix} 0 & 1 & 0 & 0 & 0 & 0 \\ 0 & 0 & 1 & 0 & 0 & 0 \\ -\dfrac{\ell(\ell+1)}{r^3} & \dfrac{\ell(\ell+1)}{r^2} & -\dfrac{3}{r} & \dfrac{\ell(\ell+1)}{r} & 0 & 0 \\ -\dfrac{\ell(\ell+1)}{r^3} & \dfrac{2}{r^2} & \dfrac{1}{r} & 0 & g(r)r & 0 \\ 0 & 0 & 0 & 0 & 0 & 1 \\ \dfrac{R_a}{r}\dfrac{\partial T_0}{\partial r} & 0 & 0 & 0 & \dfrac{\ell(\ell+1)}{r^2} & \left(-\dfrac{2}{r}+w_0\right) \end{pmatrix} \tag{18}$$

The new eigenvalue problem posed by (16) with $\underline{\underline{A}}$ given by (18) clearly has w_0 as an additional parameter.

An example of a set of neutral stability curves that is delivered by the solution of (16) as a function of the assumed convergence is shown in Figure 6. These calculations assume a basic state for the temperature profile in which the boundary layer has a thickness of 140 km which is equal to the thickness of the layer observed in Figure 4b. The results are shown for Cartesian geometry (not a serious restriction) and the outer boundaries of the domain are placed at distances away from the endothermic horizon which match those for the mantle. Inspection of the data presented on Figure 6, which are calculated for $\beta_2 = -2.8$ MPa°K^{-1}, demonstrates that as the convergence increases from zero so does the critical Rayleigh number for the shell (the convergence is specified by assuming $w_0 < 0$ above the boundary and $w_0 > 0$ below, with $|w_0|$ independent of depth). Initially, for small $|w_0|$, the neutral boundary determines a most unstable wavenumber that corresponds to a very large horizontal scale, in accord with the nature of the avalanche events described previously in connection with the discussion of Figure 2. With further increase of the convergence, the minimum on the neutral curve shifts to much higher wavenumber. Inspection of the eigenfunctions at this new minimum reveals that they possess a node in vertical velocity precisely at the phase boundary implying that the small amplitude motion

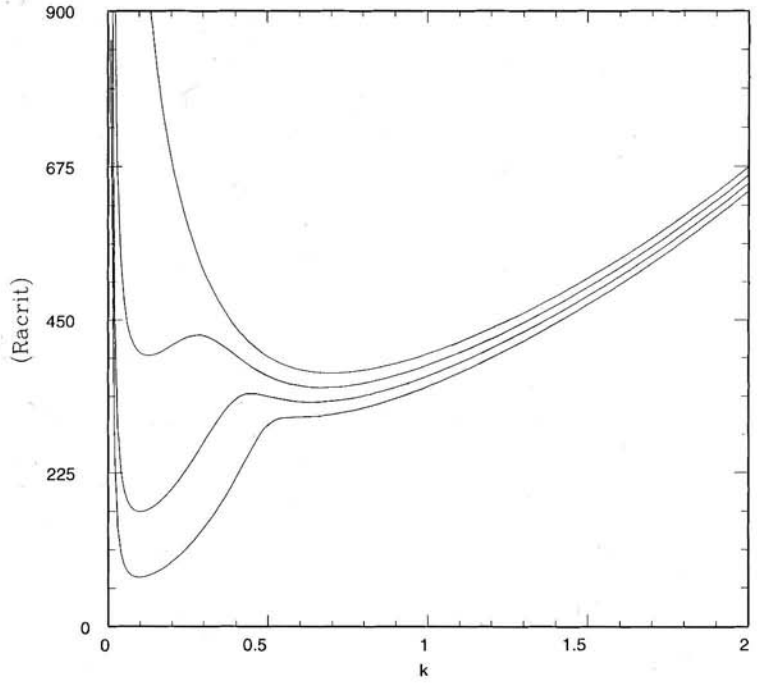

Figure 6. Neutral curves for the onset of convective instability in a plane layer of fluid containing a localized internal thermal boundary layer of the kind that develops due to the action of the endothermic phase transformation in the spherical axisymmetric model. Neutral curves are shown for several values of the "convergence" that is represented by the variable w_0 in equation (18). The four curves shown are for the respective nondimensional values 1.2, 1.3, 1.4 and 1.5 with the top most curve corresponding to the highest value of w_0.

at onset does not correspond to an instability of the entire boundary layer of avalanche type but rather to the development of separate layers of convection above and below the interface. This corresponds to a state of perfectly layered convection. This analysis therefore suggests that the intermittently layered state of flow (which obtains at a Rayleigh number of 10^7 which is equal to that of the modern earth) will obtain only in a finite range of Rayleigh number. As the Rayleigh number increases to a value outside this range and the effective radial convergence increases, the avalanche process will cease and the flow will become perfectly layered, a circumstance that was most probably, according to these analyses, characteristic of the early earth after the solidification of the mantle had occurred. Whether our calculations are truly representative of the actual earth is of course debatable as we have entirely neglected a number of effects (e.g. pressure and temperature dependence of viscosity, surface plates) which could be extremely important. Discussion of these further aspects of the problem will be provided elsewhere in due course (in part in Butler and

Peltier, manuscript in preparation). In the penultimate section below we choose to focus on a brief and largely qualitative discussion of the evidence that may be invoked to argue that the mantle convective circulation may in fact be as highly intermittent as our calculations of phase transition modulated mixing suggest. We will also briefly discuss the role that such intermittency might play in the supercontinent cycle.

4. Intermittency and the Wilson Cycle

The supercontinent cycle (often called the Wilson cycle after J. Tuzo Wilson) is a long timescale tectonic cycle which has apparently persisted through much of the post accretion evolution of the earth. It consists of intervals of continental accretion during which continental fragments are assembled to form a supercontinent, followed by intervals of "rifting" of the supercontinent which leads to the dispersal of a (perhaps new) array of such fragments. This cycle appears to be quasi-periodic with a characteristic timescale of order 0.5 Ga. The best direct evidence for the existence of the supercontinent cycle is geochemical and geochronological, an excellent example of which is shown in Figure 7, which is from the compilation of isotopic dates produced by Dearnley (1965). This shows the frequency of occurrence of radiometric date as a function of the age of the dated sample based upon approximately 3400 age determinations, a histogram which has well developed peaks (of tectonic "activity"?) at the sequence of times 2.60 Ga, 1.84 Ga, 1.09 Ga, 0.57 Ga and 0.15 Ga. The latter of these peaks is more-or-less immediately preceded by the time of onset of the breakup of the last supercontinent "Pangea". The individual peaks might reasonably be expected to correspond to epochal events in continent formation yet there has been no satisfactory explanation provided as to why such an intermittent mode of behaviour should arise. Our intention in the reminder of this section is to explore the possibility that the previously discussed influence of the endothermic phase transition on the deep convective circulation may play an important role in this process.

The dynamic process responsible for driving surface plates in their relative motion is clearly the thermally induced convective circulation that fills the Earth's mantle. The fact that this convective circulation is highly time dependent and in fact thermally chaotic (e.g. Solheim and Peltier, 1990) would naturally lead one to expect that the motion of the continents thereby produced might be chaotic as well. It seems reasonable to suppose that episodic changes in surface tectonics should be related to episodic changes in the nature of the convective circulation. Most theories that have been proposed to account for supercontinent breakup and accretion rely on some hypothesized interaction between surface plates and convection. One of the earliest qualitative theories of surface episodicity that was advanced to explain the Wilson cycle, is one which is still seen as a central tenet of the plate tectonic paradigm. According to this early view, continents are caused to rift above hot spots produced by upwelling thermal plumes and the fragments to disperse as new ocean basins form. This new ocean floor is generated at mid-ocean ridges where mantle material rises and cools as it moves laterally, leading to expansion of the basin. The oceanic lithosphere grows colder and more dense the further it migrates from the spreading center until, after reaching an age somewhat less than 200 Ma, it becomes sufficiently dense to founder and sink back into the mantle. When such "subduction" begins at a continental

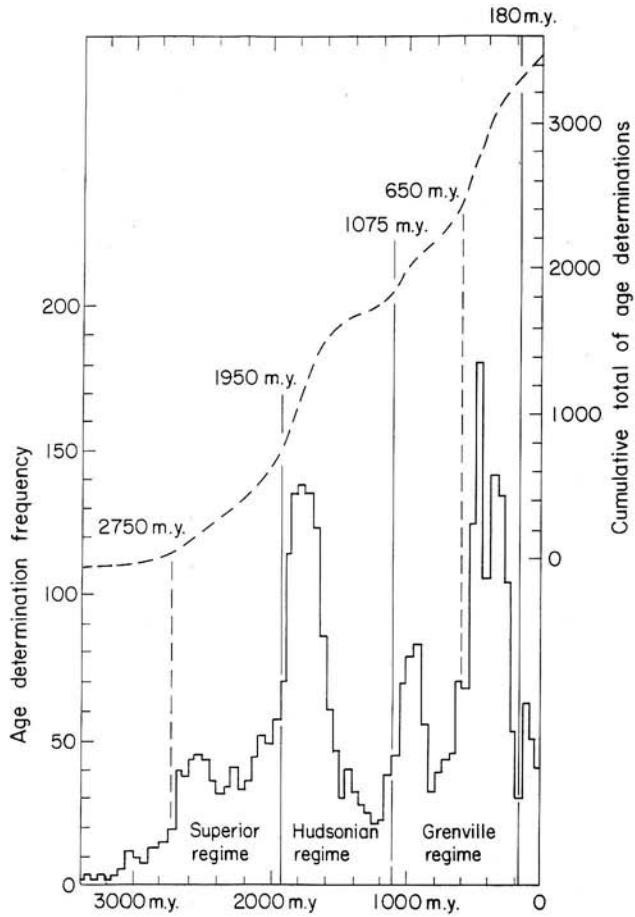

Figure 7. Histogram of the frequency of occurrence of rock age as a function of age based upon approximately 3400 isotopic age determinations (after Dearnley, 1965).

boundary, the expansion of the ocean basin ceases and the continents are thereafter supposed to accumulate once more, setting the stage for a further cycle of oceanic growth. In this qualitative picture, the surface plates are seen to be determinant of the convection pattern, imposing a rather orderly, oscillatory structure upon convection cells that is not apparent in explicit mathematical models of the mantle convective circulation. These qualitative ideas have nevertheless remained a basis for current "plate tectonic thinking" concerning the origin of the supercontinent cycle (e.g. Nance *et al.*, 1986).

Attempts to explain tectonic episodicity using a uni-phase, incompressible convection model with surface plates, run at low Rayleigh number (10^5) in 2D Cartesian geometry (e.g. Gurnis, 1988), have been based upon the notion that the plate-convection interaction

is intrinsically episodic as in the qualitative discussion above. However, due to the low Rayleigh numbers employed in these analyses, the flow pattern in the absence of plates is steady state. The addition of a surface plate perturbs the flow and produces a time dependence in which intermittent jumps in plate velocity may be observed. Aside from the fact that the parameters required to specify the nature of the plate (such as horizontal length relative to the depth of convection) determine to a large extent the observed time dependence, it is apparently the presence of the underlying steady state that is responsible for the observed episodicity which is brought on by the plate "jumping" between adjacent cell pairs. It would seem that a fundamentally different temporal behaviour would be observed if the flow, in the absence of plates, was chaotic, as is expected to be characteristic of the high Rayleigh number convective circulation of the real earth (Solheim and Peltier, 1990). Furthermore, the manner in which the plates are assumed to couple with the underlying mantle flow in these simple models may also be rather suspect.

In several prior analyses of this problem (e.g. Ichiye, 1971; Busse, 1978) it has been suggested that the presence of a supercontinent may be of itself sufficient to ensure its own eventual breakup. Thick continental lithosphere overlying an extended area of convecting mantle tends to trap heat beneath it. This causes the supercontinent to dome upward due to thermal expansion, following which there is partial melting (according to Anderson's scenario) leading to upwelling and eventually supercontinent fragmentation. The fragments thereafter disperse, emigrating from the geoid high induced at the center of the supercontinent. This is a plausible scenario for the breakup of a supercontinent, particularly since Pangea was indeed quite likely situated over the present Atlantic-African geoid high prior to its disruption (Morgan, 1981). It does not, however, offer a convincing account of the mechanism whereby the individual continental fragments initially aggregate to form a new supercontinent. It would appear that they should simply "walk" from the geoid high in a random fashion. It does not, therefore, provide a satisfactory explanation for the observed tectonic episodicity. There have been several other, equally unsatisfactory in our view, attempts to explain the long time scale quasi-periodicity that is observed in the geologic record. Since the driving force behind the surface plates is clearly mantle convection, it would appear prudent to focus more attention on this fundamental process.

In seeking to explore the extent to which our own model of the mantle convection process might provide insight into this issue we note that if the parameters of the model such as phase loop thickness, values of the Clapeyron slopes, degree of internal heating and Rayleigh number are set to lie in the "earth-like" regime, then the 660 km transition may induce significant dynamical layering with the upper mantle and lower mantle convecting separately. The layering is never complete, however, as there inevitably do exist local patches across which mass transfer occurs between the upper and the lower mantle as previously explained. Nor does the spatial pattern persist. Every 400–600 million years of dimensional time there occurs a new episode of avalanche activity across the 660 km transition at some new location or locations. The "high mass flux at 660 km" events are brought on by the growth of an instability in the internal thermal boundary layer which develops when the flow becomes layered. As discussed in the last section there is furthermore a critical boundary layer Rayleigh number based on the width of the internal boundary layer and the temperature drop across it, below which the boundary layer is stable and above which it is not, allowing a marked increase of radial mass flux in the course of the instability. Shortly

after an avalanche has fully developed, the boundary layer Rayleigh number is reduced to its previous (subcritical) value as the flux of material crossing the boundary acts to eliminate the local temperature gradient. Consequently, the internal thermal boundary layer becomes stable once more and the avalanche ceases. Individual avalanches are therefore relatively short lived events which, by their occurrence, sow the seeds of their own destruction. When such an avalanche occurs, there is an increase in surface velocity and surface heat flow as the mode of convection temporarily shifts to a predominantly whole mantle style. The massive downwelling established by the avalanche produces an area on the planetary surface directly above it which we might reasonably refer to as a "great-attractor" of surface material and in particular, we suggest, of continental fragments. Continental fragments would accumulate at this point to form a new supercontinent. The avalanche at 660 km is arrested after 100 or 200 Ma and the convection pattern thereafter returns to a dominantly layered style. This layered style of convection typically persists for a further 300–400 million years. During this time of relative quiescence, the supercontinent will be gradually broken up by the continued action of small scale upper mantle convection beneath it and the continental fragments so produced will be scattered by the underlying flow. Eventually, a further major avalanche event will occur and once more gather the continental fragments together that lie within its attractor basin. It should be clear that there may in general be more than a single avalanche occurring in any given epoch. However, only a single event or pair of events every few hundred million years is sufficiently intense, according to the scenario we are sketching here, to cause significant change in the average absolute surface velocity (see below) and therefore sufficient to act as a "great-attractor" of widely dispersed continental fragments.

To establish the plausibility of the above described scenario through quantitative analysis we show, in Figure 8, time series of the average absolute value of the mass flux at 660 km depth (frame A), the average absolute surface velocity (frame B) and the Nusselt number (frame C) over a period of 1.25 Ga from a typical high resolution simulation of the convection process. These time series were produced from a simulation in which the Rayleigh number is 10^7, there is internal heating corresponding to roughly 50% heating from within and 50% heating from below, the Clapeyron slope of the 410 km phase transition is +3.0 MPa/°K, the Clapeyron slope of the 660 km transition is –2.8 MPa/°K and the radial extent over which both phase transitions take place is 25 km (25 km thick phase loops). These parameter values fall within the "earth-like" range excepting that for the phase loop thicknesses which are somewhat large but nevertheless adequate to capture the dynamical influence of the phase boundaries properly. The time series in Figure 8 indicate the occurrence of three intense avalanche events over the period shown for these mean fields, one at the beginning, one in the middle and one at the end of the time interval. Each event is characterized by an abnormally high 660 km average mass flux (frame A). Associated with these events are significant increases in the average surface velocity and surface heat flow (surface heat flow is directly proportional to the Nusselt number). As is apparent from Figure 8 there is a major avalanche of upper mantle material across the 660 km horizon that significantly impacts the mean fields approximately every 0.5 Ga, the approximate timescale separating epochs of continental crustal rock formation inferred on the basis of Figure 7. The average surface velocity and Nusselt number, however, exhibit smaller amplitude excursions from the "mean" on shorter timescales which has the effect of making the major events less well defined in the time series of frames B and C.

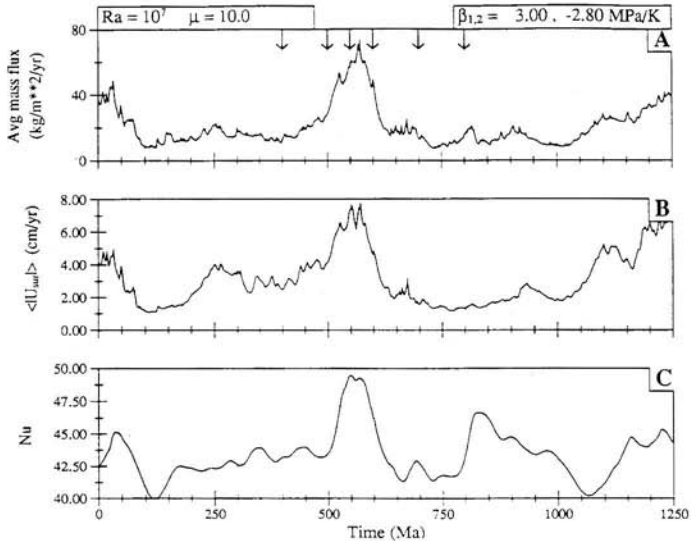

Figure 8. Time series of the average absolute mass flux at 670 km depth (plate A), the average absolute value of the surface velocity (plate B) and the surface Nusselt number (plate C). These time series come from a simulation in which the parameters were set to be in the "earth-like" range (see text) and reveal three major episodes of avalanche activity at the beginning, middle and end of the time period respectively. The arrows in plate A indicate the times at which the temperature fields are shown in Figure 9.

In order to understand the possible consequences of the above described avalanche phenomenon for the problem of tectonic episodicity it will prove useful to examine one "high mass flux at 660 km" event in detail. To this end we show in Figure 9 the instantaneous temperature fields at six different times through the event centred on 500 Ma for the times denoted by the arrows. The first field at 400 Ma corresponds to a state that exists just prior to the major avalanche event and, as is apparent from the image shown, the mantle circulation is strongly layered at this instant of time. There is some localized mass flux across the 660 km horizon that is occurring near the lower pole but it is not sufficiently intense to affect the global average (see Figure 9). It does, however, have an effect on the average surface velocity and heat flow. As is apparent in Figure 8, the surface velocity and heat flow are increased for a period of roughly 300 Ma prior to the main avalanche event beginning at 500 Ma. This is a consequence of a relatively weak descending plume that is migrating toward the lower pole, the same plume that is evident in the 400 Ma and 500 Ma frames of Figure 9, but which has disappeared completely by 600 Ma. This relatively large, but not extremely vigorous descending plume tends to increase the average absolute velocity at the surface and consequently the average heat flow through the surface. It does not do so on the scale of the major mass flux event which is about to occur, however. Between 450 Ma and 500 Ma of model time another large scale sinking plume begins to emerge (Figure 9).

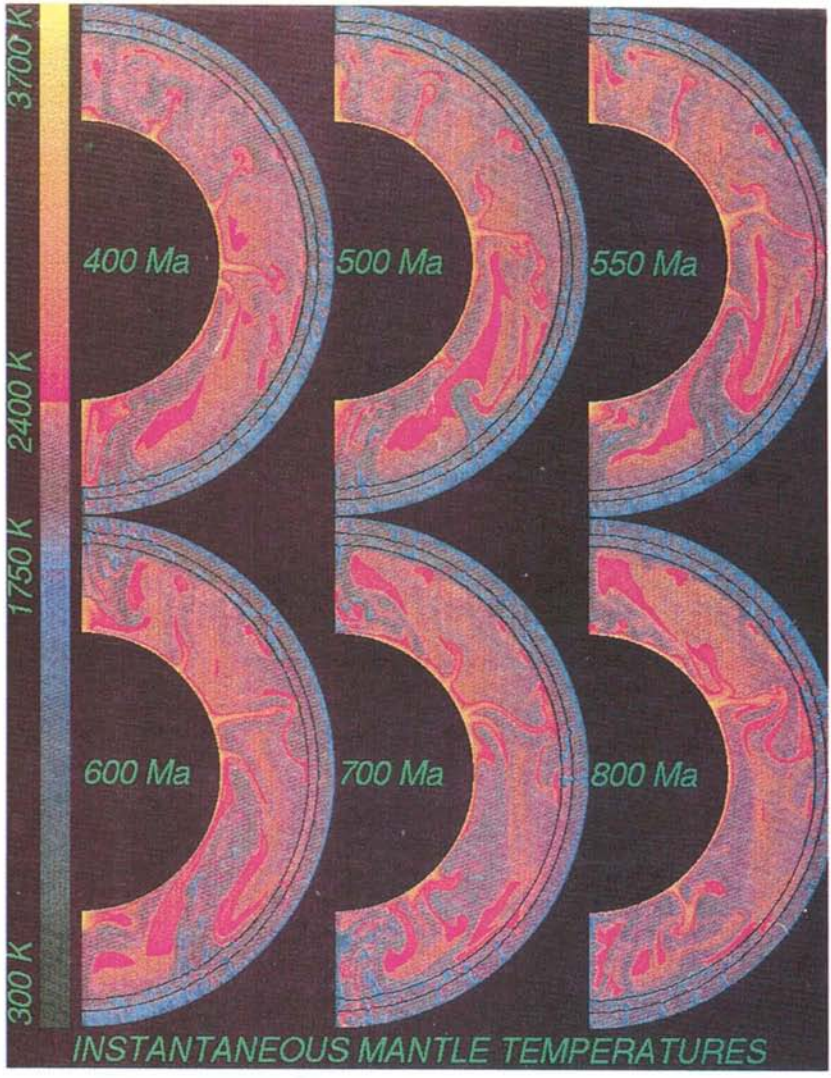

Figure 9. Six temperature fields from the simulation for which diagnostic time series were presented in Figure 8 and the times indicated by the arrows in that figure. This sequence illustrates the evolution of the temperature field through one major episode of avalanche activity.

It originates from a position 40 degrees from the lower pole and grows rapidly in intensity for the next 100 Ma. At approximately the same time an avalanche is beginning at the uppermost pole which will endure until approximately 700 Ma of model time. These are the events which combine to produce the anomalously high mass flux observed in Figure 8. The former plume travels toward the south pole reaching a peak in intensity between 550 Ma

and 600 Ma but is almost exhausted by 700 Ma (Figure 9). By the final frame (800 Ma) the flow is once again almost perfectly layered. At this time none of the descending material is able to penetrate the 660 km boundary and there is, therefore, a tendency for it to accumulate at this depth. Similarly, lower mantle material is unable to ascend through the 660 km horizon and there are pockets of anomalously hot material accumulating just below this boundary. These circumstances lead to an increase in the temperature drop across the internal thermal boundary layer that has developed at 660 km. Ultimately this will cause the local internal boundary layer Rayleigh number to exceed its critical value as discussed previously and a further avalanche event will ensue. The high mass flux event in the mean fields that occurs between 450 Ma and 650 Ma of model time is therefore the result of two concurrent avalanches of fluid at 660 km. The net effect of these two avalanches is to establish a mantle wide circulation pattern. In this case there are two major cells with downwellings at the north pole and 30 degrees from the south pole and an upwelling at 80 degrees from the north pole. There is a smaller cell pair between the south pole and the major downwelling 30 degrees distant. Such large scale global mixing only occurs during the high mass flux events. Little communication between upper and lower mantle occurs at intermediate times.

Surface velocity as a function of meridional location can then be a useful diagnostic of whole mantle or layered convection and is in any event vital to developing an understanding of the impact that such events will have on continental material. Figure 10 displays the surface velocity as a function of angular position along the surface (θ) for four of the temperature fields depicted in Figure 9. The four fields selected correspond to the times shown in the upper left hand corner of each frame. Frame A illustrates the surface velocity at 500 Ma, just at the beginning of a major mass flux event. We note that over a large portion of the surface the velocity is relatively large and negative (indicating motion toward the lower pole at $\theta = 0$). Over the remainder of the surface the velocity hovers near zero. The large extent of the region of negative surface velocity indicates that a large expanse of the surface from 30 degrees to 110 degrees is moving coherently towards the south pole (at 500 Ma). This expanse of surface material is moving toward a point of massive subduction brought on by the avalanche that is occurring at 30 degrees from the south pole (see Figure 9). Between 500 Ma and 600 Ma another avalanche begins to form at the north pole. This event also attracts material towards it. We note in frame B of Figure 10 that the surface velocity as a function of position along the surface is essentially bimodal, indicating massive movement branching north and south along the surface from about 110 degrees. Figure 9 indicates that this is the location of a major upwelling that originates at the core-mantle boundary. At this point in time, the mantle is convecting as two major, mantle wide cells extending from the north pole to roughly 30 degrees from the south pole. The convection pattern between the south pole and 30 degrees is rather complex at this instant of time but in general surface material (and, implicitly, continental fragments) is moving toward the south pole. After the avalanches have subsided the surface velocity decreases on average and there is no distinct pattern that is apparent in the later frames C and D of Figure 10. Surface velocity thereafter fluctuates about zero, a consequence of the small scale convection cells that operate near the surface in the layered convection state (see the 700 Ma and 800 Ma plates of Figure 9). We therefore note that the high mass flux events clearly evident in Figure 8, which are characterized by high average absolute surface velocities and high average surface heat flow, are indicators of the fact that the pattern of convection has shifted temporarily from a layered to a whole

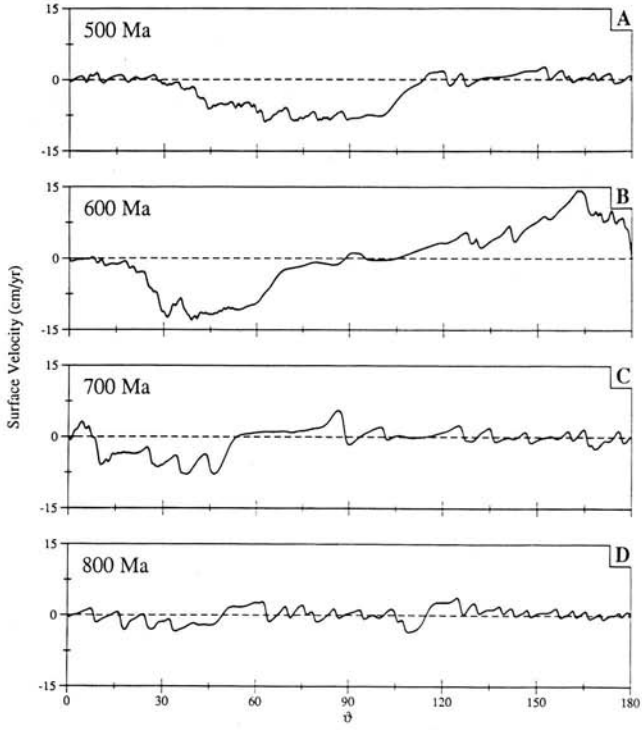

Figure 10. Frames A through D illustrate the evolution of the surface velocity field through the avalanche event illustrated by the temperature fields shown on Figure 9. Negative tangential velocity denotes material motion in the direction of the pole at $\theta = 0$, positive away. In frames A and B the avalanche event is active whereas in frames C and D it has subsided. During the avalanche event surface material, even at large distances removed from the avalanche, moves towards the point on the surface above the 670 km downwelling (note especially frame B). After the avalanche has subsided the coherence of the surface motion disappears.

mantle style. When these avalanches occur, they induce "super" subduction zones above them which attract surface material toward them from a great distance. Once the avalanche has abated, average surface velocity decreases dramatically and large scale coherence is lost as surface motions revert to the small scale typical of layered convection.

Continents form a part of the complex outer layer of crust that surrounds the planetary mantle. When one of these high mass flux events occurs and one or more "super" subduction zones develop at the surface, continental fragments will tend to accumulate above the region of massive downwelling. If an average velocity of 6 cm/yr (see Figure 2) is maintained within the attractor basin of an avalanche for 150 Ma then continental fragments as distant as 9000 km could be collected to form the supercontinent. When the supercontinent has formed and the avalanche subsides, the stage is set for the supercontinent to break up. The

large surface area covered by the insulating continental crust (as in the Busse and Anderson scenario) will tend to trap the heat delivered to it by underlying small scale upper mantle convection. This will cause the continental lithosphere to dome upwards and eventually to rift. The small scale convection cells operating in the upper mantle at this time will then be able to separate the fragments so produced. The fragments will separate in a complex fashion directed by their interaction with the upper mantle circulation. Their average velocity will be much less than that which obtains during the avalanche event (perhaps 2–4 cm/yr based on Figure 2). Consequently, they will not likely migrate far before the next avalanche event at 660 km depth occurs in their general vicinity (likely within the first few hundred million years following rifting, according to our analysis. When this event occurs, the fragments will once more accumulate to create a supercontinent and the cycle will repeat.

5. Conclusions

We have clearly established that there exists a long timescale episodicity in axisymmetric spherical convection that is characteristic of the convection process in a multi-phase, mantle like fluid, that might help considerably to explain major aspects of the Wilson cycle of supercontinent formation and destruction that is revealed in the geological record. The mantle convects in a radially layered fashion in general but every few hundred million years there occurs a sufficiently intense avalanche of material across the 660 km boundary that a mantle wide convection pattern is temporarily induced. Associated with this mantle wide mode of convection is abnormally high surface velocity and the presence of one or more major attractor basins at the surface into which continental fragments may be accumulated from a distance of many thousands of kilometres. These continental fragments accumulate to form a supercontinent. The avalanches are typically arrested according to our calculations after 100–200 Ma and a predominantly layered style of convection is thereafter restored. The insulating supercontinent so created will accumulate heat beneath it which will eventually cause it to rift and the underlying upper mantle circulation will thereafter separate the continental fragments once again. The characteristic time that separates major avalanche events is not accurately constrained by our own simple axisymmetric model and is likely highly variable consistent with Figure 7. It will be affected by varying model parameters such as Rayleigh number, the fractional heating from within and by temperature and pressure dependent viscosity and the influence of surface plates. Increasing the Rayleigh number tends to promote layering (e.g. Solheim and Peltier, 1993) and therefore to reduce the number of avalanche events that will occur within a given time. Since the Rayleigh number in the early earth was likely much higher than its present value, near 10^7, this could be significant. The effect of full three dimensionality is also important. There is some recent indication that, at least at much lower Rayleigh numbers (near 10^6), the incidence of avalanches is increased in three dimensions (Tackley *et al.* 1994). Since the introduction of three dimensionality may have an effect that is opposite to raising the Rayleigh number, it is at present unclear which influence will be found to dominate when a 3D spherical model is run at earth-like Rayleigh numbers. Adding surface plates to the model may also affect the characteristic time scale of these events as will the influence of pressure and temperature dependent viscosity. This will not influence the avalanche process directly, however, because

the process is driven by the growth and decay of instabilities in the internal thermal boundary layer at 660 km depth, as we have shown. The fundamental mechanism that underlies the episodicity discussed here may prove relatively robust, however, and detailed analysis of the various effects that we have omitted may be found to leave the basic theory advanced here essentially unaffected insofar as qualitative behaviour is concerned. Whether or not this expectation will be realized is a question that we expect will be answered in the course of continuing analyses by ourselves and others. In this work we expect that the question of the manner in which the Garnet component of the upper mantle mineralogy transforms with increasing pressure from the transition zone into the lower mantle may become critical. If this 40% by composition component of the bulk mineral assemblage were to transform with less negative (or perhaps positive) Clapeyron slope then it is conceivable that the propensity of the endothermic transformation of the Spinel phase to induce layering could be reduced. This issue is a subject of current investigation.

6. References

Akimoto, S., and H. Fujisawa, Olivine-spinel transitions in the system Mg_2SiO_4-Fe_2SiO_4 at 800°C. *Earth Planet. Sci. Lett.*, **1**, 237–240 (1966).

Busse, F.H., *Geophys. J. R. Astr. Soc.*, **53**, 1 (1978).

Busse, F. and G. Schubert, Convection in fluid with two phases. *J. Fluid Mech.*, **46**, 801–812 (1971).

Cathles, L.M., The viscosity of the Earth's mantle, Princeton University Press, Princeton, N.J. (1975).

Christensen, U.R. and D.A. Yuen, The interaction of a subducting lithospheric slab with a chemical or phase boundary. *J. Geophys. Res.*, **89**, 4389–4402 (1984).

Christensen, U.R. and D.A. Yuen, Layered convection induced by phase transitions. *J. Geophys. Res.*, **90**, 10,291–10,300 (1985).

Dearnley, R., *Nature*, **206**, 1083 (1965).

Gurnis, M., Large-scale mantle convection and the aggregation and dispersal of supercontinents. *Nature*, **332**, 695–699 (1988).

Honda, S., D.A. Yuen, S. Balachandar and D. Reuteler, Three-dimensional instabilities of mantle convection with multiple phase transitions. *Science*, **259**, 1308–1311 (1993).

Howard, L.N., Proc. 11th Int. Cong. in Applied Mech. (Munich, 1964) H. Goertler ed. p. 1109, Berlin (1966).

Ichiye, T., *J. Geophys. Res.*, **76**, 1139 (1971).

Ito, E. and E. Takahashi, Post-spinel transformations in the system Mg_2SiO_4-Fe_2SiO_4 and some geophysical implications. *J. Geophys. Res.*, **94**, 10,637–10,646 (1989).

Jeanloz, R. and A.B. Thompson, Phase transition and mantle discontinuities. *Rev. Geophys.*, **21**, 51–74 (1983).

Machetel, P. and P. Weber, Intermittent layered convection in a model mantle with an endothermic phase change at 670 km. *Nature*, 55–57 (1991).

Morgan, W.J., in The Sea, C. Emiliani, Ed. (Wiley-Interscience, New York), **7**, pp. 443–488 (1981).

Nance, R.D., T.R. Worsley and J.B. Moody. *Geology*, **14**, 514 (1986).

O'Nions, R.K., N.M. Evenven and P.J. Hamilton, Geochemical modelling of mantle differentiation and crustal growth. *J. Geophys. Res.*, **84**, 6091–6101 (1979).

O'Nions, R.K. and I.N. Tolstikhin, Behaviour and residence times of lithophile and rare gas tracers in the upper mantle. *Earth and Planet. Sci. Lett.*, **124**, 131–138 (1994).

Peltier, W.R., Penetrative convection in the planetary mantle. *Geophys. Fluid Dyn.*, **5**, 47–88 (1972).

Peltier, W.R., The impulse response of a Maxwell Earth. *Rev. Geophys. Space Phys.*, **12**, 649–669 (1974).

Peltier, W.R., Mantle convection and viscoelasticity. *Annu. Rev. Fluid Mech.*, **17**, 561–608 (1985).

Peltier, W.R. and G.T. Jarvis, Whole mantle convection and the thermal evolution of the Earth. *Phys. Earth Planet. Inter.*, **29**, 281–304 (1982).

Peltier, W.R., Mantle convection and viscoelasticity. *Annu. Rev. Fluid Mech.*, **17**, 561–608 (1985).

Peltier, W.R. and G.T. Jarvis, Whole mantle convection and the thermal evolution of the Earth. *Phys. Earth Planet. Inter.*, **29**, 281–304 (1982).

Peltier, W.R. and L.P. Solheim, Mantle phase transitions and layered chaotic convection. *Geophys. Res. Lett.*, **19**, 321–324 (1992).

Richter, F.M. and D.P. McKenzie, On some consequences and possible causes of layered mantle convection. *J. Geophys. Res.*, **86**, 6133–6142 (1981).

Ringwood, A.E. and A. Major, The system Mg_2SiO_4-Fe_2SiO_4 at high pressures and temperatures. *Phys. Earth Planet. Inter.*, **3**, 89–108 (1970).

Schubert, G., D.A. Yuen and D.L. Turcotte, Role of phase transitions in a dynamic mantle. *Geophys. J.R. Astron. Soc.*, **42**, 705–735 (1975).

Solheim, L.P. and W.R. Peltier, Heat transfer and the onset of chaos in a spherical, axisymmetric, anelastic model of whole mantle convection. *Geophys. Astrophys. Fluid Dyn.*, **53**, 205–255 (1990).

Solheim, L.P. and W.R. Peltier, Mantle phase transitions and layered convection. *Can. J. Earth Sci.*, **30(5)**, 881–892 (1993).

Solheim, L.P. and W.R. Peltier, Avalanche effects in phase transition modulated thermal convection: A model of Earth's mantle. *J. Geophys. Res.*, **99**, 6997–7018 (1994a).

Solheim, L.P. and W.R. Peltier, Phase boundary deflections at 660 km depth and episodically layered isochemical convection in the mantle. *J. Geophys. Res.*, **99**, 15,861–15,875 (1994b).

Tackley, P.J., D.J. Stevenson, G.A. Glatzmeier and G. Schubert, Effects of an endothermic phase transition at 670 km depth on spherical mantle convection. *Nature*, **361**, 699–704 (1993).

Tackley, Paul J., D.J. Stevenson, G.A. Glatzmeier and G. Schubert, Effects of multiple phase transitions in a three-dimensional spherical model of convection in Earth's mantle. *J. Geophys. Res.*, **99**, 15,877–15,901 (1994).

Wasserburg, G.J. and D.J. DePaulo, Models of earth structure inferred from Neodymium and Strontium isotopic abundances. *Proc. Natl. Acad. Sci. USA*, **76**, 3594–3598 (1979).

Weinstein, S.A. Catastrophic overturn of the Earth's mantle driven by multiple phase changes and internal heat generation. *Geophys. Res. Lett.*, **20**, 101–104 (1993).